Available online at www.sciencedirect.com
SCIENCE DIRECT®
Cement & Concrete Composites 27 (2005) 716–726
Cement & Concrete Composites
www.elsevier.com/locate/cemconcomp

A simplified isotropic damage model for concrete under bi-axial stress states

Xiaoya Tao *, David V. Phillips

Department of Civil Engineering, University of Glasgow, Glasgow G12 8LT, UK

Received 30 May 2003; accepted 8 September 2004

Abstract

This paper presents a concrete model that is capable of describing the response of concrete under bi-axial loading, with the features of simplicity and avoidance of convergence problems, often seen in plasticity based models. The proposed model incorporates the failure of concrete into a conventional continuum damage mechanics framework, where particular emphasises are placed on highlighting the different responses of concrete under tension and compression, as well as the different contributions of hydrostatic and deviatoric stress components on concrete damage. A weighted damage parameter and a damage multiplier are introduced to eliminate potential convergence problems and to reduce the effect of hydrostatic pressure on damage, respectively. Finally, several examples are provided and compared with experimental data.

Keywords: Concrete model; Isotropic damage; Bi-axial loading; Finite element analysis

1. Introduction

The mechanical response of concrete is weakened by the development of micro-cracks and is mainly characterised by strain softening, progressive deterioration, volumetric dilatancy, and induced anisotropy. From plasticity, damage and fracture mechanics viewpoints, these phenomena can be considered as a combination of unrecoverable plastic deformation, the degradation of material stiffness and the nucleation, growth and interaction of those defects, presented in Fig. 1 for uniaxial loading. In order to model the complicated responses of concrete-like materials, different mechanics theories can be adopted. In general, to determine plastic deformation classical plasticity theory is effective; to describe strain-softening, one can use either plasticity theory or continuum damage theory; to simulate crack opening and closure, fracture mechanics, plasticity and contact methods can be employed. However, the simplest and most effective method to model stiffness degradation is through continuum damage mechanics, which assumes cracking reduces the Young's modulus of the material.

Various damage mechanics based methods for modelling the response of concrete have been developed and various mechanisms for describing its behaviour have been suggested. Amongst these are plastic-damage models [1–4], coupled elastoplastic-damage models [5–11], and friction-damage models [12–16], to mention just a few. In the plastic-damage approach, the thermodynamic potential is decomposed into two parts. One is related to elastic behaviour and the other to plastic response. The latter may be modelled by either plasticity theory or by directly introducing a plastic term that is associated with a damage internal variable, such as in the work of La Borderie et al. [4]. In the coupled

* Corresponding author. Tel.: +44 797 0672882.
E-mail address: xyt0629@hotmail.com (X. Tao).

0958-9465/$ - see front matter © 2004 Elsevier Ltd. All rights reserved.
doi:10.1016/j.cemconcomp.2004.09.017

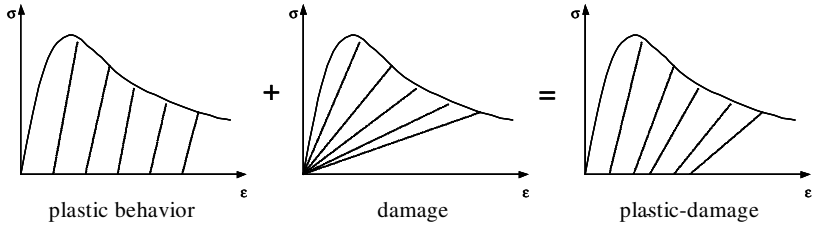

Fig. 1. Plastic-damage behaviour of concrete materials.

elastoplastic-damage model, the concept of stiffness degradation is coupled with classical plasticity theory. As for friction-damage models, micro-crack growth is coupled with friction related to dissipative mechanisms. The friction sliding over internal crack surfaces is assumed to have a plasticity kind of behaviour. However, among these, a proper description of strain softening and stiffness degradation by means of damage mechanics is essential.

The application of continuum damage mechanics theory to concrete dates from the late 1970s. Typically, these include the scalar damage models [17], unilateral damage models [12,18], models with permanent strains, induced anisotropy or high compressive stresses [19,13], models which include anisotropic damage and dilation [3,20], as well as thermo-mechanical damage [21,22]. Among the various scalar damage models, Mazar's is perhaps more popular due to its simplicity.

Generally, a typical reverse cyclic loading on concrete may be described by six stages, see Fig. 2, i.e. elastic tension upon yielding (segment ab), subsequently tensile hardening/softening (segment bc), then elastic unloading (segment cd); once into compressive state, starting with compressive loading until yielding (segment de), then compressive hardening/softening (segment ef), finally reverse unloading (segment fg). Corresponding to these processes, concrete experiences changes from initiation/nucleation of micro-cracks, propagation and clustering

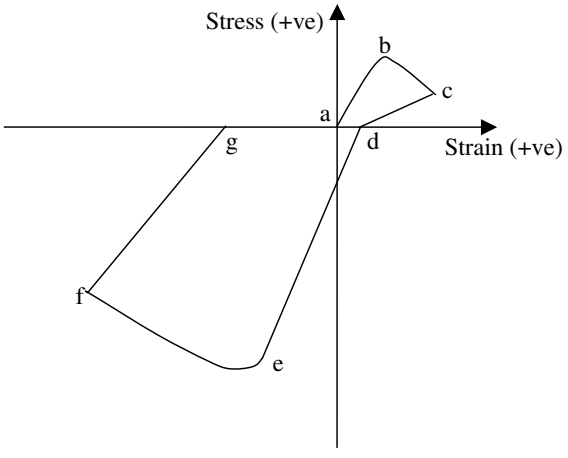

Fig. 2. Typical concrete response under reverse uniaxial tensile/compressive loading.

of existing cracks, crack closure under unloading process, moduli recovery under compressive loads (unilateral effect), and partial crushing. From a damage mechanics standpoint, they can be simply described as (1) degradation of stiffness by a tensile damage parameter; (2) hardening/softening of tensile damage surface by a proper hardening/softening parameter, i.e. an evolution law related to tensile strain or stress; (3) elastic unloading with constant stiffness; (4) stiffness recovery by activating compressive damage parameter; and then (5) hardening/softening of compressive damage surface and stiffness degradation controlled by another evolution law related to compressive strain or stress; and finally (6) compressive unloading with constant stiffness.

How to activate and inactivate tensile and compressive damage evolution laws is a key issue, which requires information on tensile/compressive stress/strain state. A common practice is to separate stress and strain into positive and negative parts in some existing models. Tensile and compressive damage are independently calculated by means of corresponding damage parameters with the change in load. This treatment is feasible and reasonable for monotonic uniaxial loading where only one of damage surfaces (tensile or compressive) dominates damage evolution. However, convergence problems would arise under bi-axial and reverse cyclic loading, or even uniaxial reverse cyclic loading due to the conflict of tensile and compressive damage surfaces induced by the Poisson's ratio effect. In a uniaxial reverse cyclic loading case, for instance, tensile damage may (quickly) exceed the major compressive damage due to transverse expansion under compression, which, in turn, may result in a wrong judgement for activating tensile or compressive evolution laws and lead to premature convergence difficulties.

The model introduced in this paper is motivated by the problem encountered in modelling pullout response of fibre reinforced concrete by classical plasticity theory, where severe spalling of cement matrix may cause convergence problem. It is required to develop a bi-axial isotropic concrete model, with the principle of being simple (e.g. a few parameters and little computing complexity) and easy to implement in existing commercial FE packages, but with less convergence problems. In the contribution, we start with a simple outline of the damage mechanics framework, and then follow by

formulating and elucidation of the model, where two damage variables are introduced to cater for the requirement of different damage criteria for tension and compression. In addition, the interaction between tensile and compressive damage under bi-axial and reverse cyclic loading is coped with by weighting the two damage variables according to Mode I cracking assumptions. The weighted damage variable automatically plays a role in separating the stress into positive and negative parts, avoiding conflict between tensile and compressive damage surfaces and improving convergence of numerical computations. Based on the experimentally observed response of concrete [7], it is assumed that the spherical and deviatoric components of the principal strain/stress tensor have different contributions to damage, then a damage multiplier is designed to reduce the effect of the hydrostatic component on damage. Finally, the model is validated by several examples. Some special applications can be found in Refs. [23,24] for the damage of cement in the pullout of fibre/bar reinforced cement composites.

The main benefits of the proposed damage model are that (i) it avoids the computational complexities caused by separating strain/stress into positive and negative parts to consider different damage in tension and compression; (ii) it uses a weighted damage parameter that remedies the anomaly and the potential convergence problems due to the conflict of tensile and compressive damage surfaces under bi-axial or cyclic loading; (iii) the implementation of the proposed model in finite element code can be simplified by a description of potential energy in strain space.

2. Damage mechanics framework

Continuum damage mechanics (CDM), pioneered by Kachanov [25], is based on the thermodynamics of irreversible processes and relevant assumptions, such as the homogenisation concept, the internal state variable theory and the kinetic law of damage growth. In damage mechanics, a discontinuous material under cracking is treated as a continuum and its non-linear response is described in a straightforward manner by means of damage parameters. The advantages of damage mechanics are that one can arbitrarily choose the admissible potential forms, which satisfy the first principle of thermodynamics and equations of damage growth in order to achieve the best fit to experimental data [19].

Consider a deformable body under a static loading and subjected to progressive damage. The elastic energy per unit volume, U, of the body is a function of the elastic strain tensor ε, entropy η and an internal damage variable D, i.e.

$$U(\varepsilon,\eta,D) = (1-D)U^0(\varepsilon,\eta) \tag{1}$$

where $U^0(\varepsilon,\eta)$ is elastic energy of the virgin (undamaged) material.

The damage variable D may be a scalar or a tensorial quantity. The scalar representation implies that the damage is isotropic and ignores the influence of the orientation of micro-defects. Within the domain of D ($0 \leqslant D \leqslant 1$), $D = 0$ means that the material is undamaged, whilst $D = 1$ denotes complete fracture.

To derive a family of thermodynamic constitutive relations, the second law of thermodynamics is fundamental. From this law, the Clausius–Duham Inequality for the irreversible process (not necessarily adiabatic) is given by

$$\dot{\eta} - \nabla\left(\frac{Q}{\Theta}\right) \geqslant 0 \tag{2}$$

where Q is heat flux, i.e. dissipation of mechanical energy, Θ is temperature and ∇ is a gradient operator.

According to the first law of thermodynamics, the change of internal energy in concrete (supposing that no kinetic and potential energies exist) is written as

$$\dot{U} = \sigma : \dot{\varepsilon} + \dot{Q} \tag{3}$$

with σ the stress tensor and

$$\dot{U} = \frac{\partial U}{\partial \varepsilon}\dot{\varepsilon} + \frac{\partial U}{\partial D}\dot{D} + \frac{\partial U}{\partial \eta}\dot{\eta} \tag{4}$$

Substituting Eqs. (3) and (4) into Eq. (2), we have

$$\left(\Theta - \frac{\partial U}{\partial \eta}\right)\dot{\eta} + \left(\sigma - \frac{\partial U}{\partial \varepsilon}\right)\dot{\varepsilon} - \frac{\partial U}{\partial D}\dot{D} - Q\frac{\dot{\Theta}}{\Theta} \geqslant 0 \tag{5}$$

For an isothermal (slow loading and slow cracking growth) and elastic system, $\dot{D}$ is independent of $\dot{\eta}$ and $\dot{\varepsilon}$. In order that the inequality holds for arbitrary $\dot{\eta}$ and $\dot{\varepsilon}$ in a given thermo-dynamic state, it is required that

$$\Theta = \frac{\partial U}{\partial \eta} \tag{6}$$

$$\sigma = \frac{\partial U}{\partial \varepsilon} \tag{7}$$

$$\frac{\partial U}{\partial D}\dot{D} = Y\dot{D} \leqslant 0 \tag{8}$$

where Y is a thermodynamic force (damage energy release rate). In other words, it is an amount of dissipated internal energy for generating unit damage, a measure of damage susceptibility. The physical interpretation of Eq. (8) is that the damage process reduces the internal energy of a system.

Two other forms of free energy are often adopted in the application of damage mechanics, i.e. Helmholtz free energy per unit volume, A, and Gibbs free energy per unit volume, G. Generally, the Helmholtz free energy uses displacement as the independent variable, while the Gibbs free energy uses force as the independent variable. They are respectively defined as follows [3]:

$$A(\varepsilon,\Theta,D) = U(\varepsilon,\eta,D) - \Theta\eta \tag{9}$$

$$G(\sigma,\Theta,D) = \sigma : \varepsilon - A(\varepsilon,\Theta,D) \tag{10}$$

The Helmholtz free energy is strain energy, whilst Gibbs' is the complementary of the Helmholtz free energy. The model described here uses Helmholtz free energy from which we have

$$\eta = -\frac{\partial A}{\partial \Theta} \tag{11}$$

$$\sigma = \frac{\partial A}{\partial \varepsilon} \tag{12}$$

$$\frac{\partial A}{\partial D}\dot{D} \leqslant 0 \tag{13}$$

To determine stress or strain states during a damage process from the thermodynamic constitutive relations Eqs. (6)–(8) or Eqs. (11)–(13) a damage surface and its evolution law have to be specified. Referring to the definitions of a yield function and plastic flow law in plasticity theory, we define, for an isothermal process, the damage surface f as a function of the thermodynamic force Y and the damage parameter D, with a similar form to that of La Borderie et al. [4].

$$f(Y,D) = Y - Y^0 - Z = 0 \tag{14}$$

where Y^0 is an initial damage threshold which governs the onset of damage. As damage progresses, the initial damage surface changes by means of an evolution law defined by a hardening/softening parameter Z. Z can be expressed mathematically in different forms, such as polynomials, power and exponential functions etc. Amongst them power and exponential have the best match for the shapes of loading curves of concrete. Here, we assume that the softening of a damage surface follows a power law in the form of

$$Z = \frac{1}{a}\left(\frac{D}{1-D}\right)^{1/b} \tag{15}$$

in which a and b are two material constants to be calibrated by means of uniaxial tensile and compressive experiments of concrete. The effects of a and b on Z as damage progress are illustrated in Fig. 3. It shows that the shape of damage surface varies with b, whilst a determines the magnitude of Z. In other words, parameter a mainly dominates the magnitude of damage surface with units of MPa^{-1}, whilst b, a dimensionless parameter, influences generally the characteristics of softening/hardening (see Fig. 4 for explanation). A proper

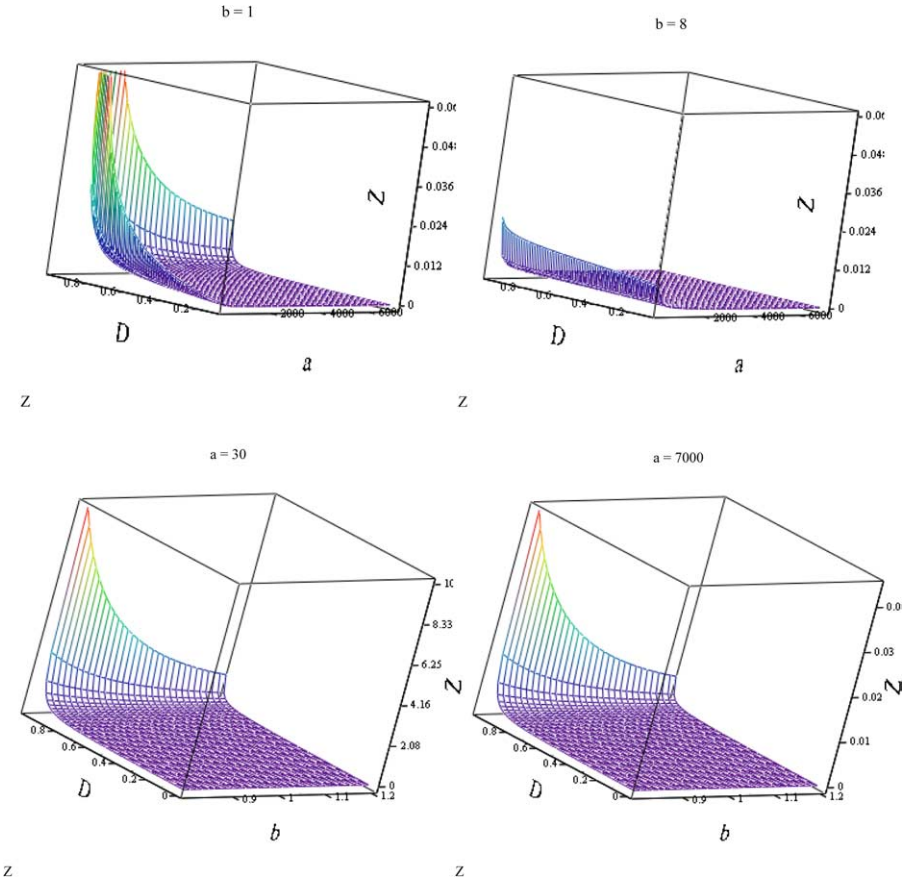

Fig. 3. Effects of a and b on Z.

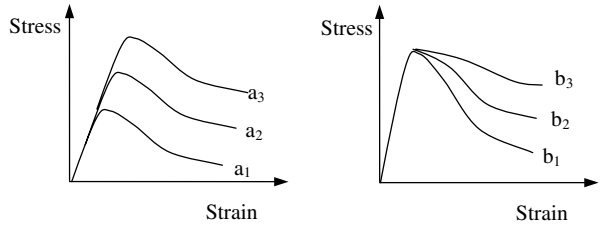

Fig. 4. Physical meanings of a and b.

selection of parameters a and b tailors Z to the demands of different types of concrete and their tensile and compressive strengths.

Consequently, the damage parameter is derived from Eqs. (14) and (15) as

$$D = 1 - \frac{1}{1 + [a(Y - Y_0)]^b} \tag{16}$$

A stress point in principal stress space can be either within or on the current damage surface. When within the damage surface, the stress point may be loading, but it has not violated the current damage criterion yet. Once it is on the damage surface, two damage states exist. One may be unloading or neutral loading, having $\dot{D} = 0$. The other is loading, accompanied by the evolution of damage and defined as $\dot{D} > 0$. Mathematically, the above description is written as

$$\begin{array}{llll} \text{if} & f < 0 & \text{then} & \dot{D} = 0; \\ \text{if} & f = 0 \text{ and } \dot{f} \leqslant 0 & \text{then} & \dot{D} = 0; \\ \text{and} & \text{if } f = 0 \text{ and } \dot{f} > 0 & \text{then} & \dot{D} > 0. \end{array} \tag{17}$$

Conditions (17) are the classical Kuhn–Tucker conditions extended to damage.

3. A bi-axial damage model for concrete

Based on the damage mechanics framework, a bi-axial damage model for concrete is now developed, where the indexes *ijkl* and *uvst* will be associated with the variables in the component stress/strain space, while *p* be related to those in the principal stress/strain space.

3.1. Potential function

Under isothermal conditions, the simplest form of a Helmholtz free energy can be written as

$$A = \frac{1}{2}\varepsilon_{uv} K_{uvst} \varepsilon_{st} \tag{18}$$

where K_{uvst} is the constitutive tensor of a material, and ε_{uv} (or ε_{st}) is a strain tensor.

Experimental evidence demonstrates that the susceptibility of concrete to damage and failure is different under pure hydrostatic loadings from deviatoric loadings. In order to distinguish the different contributions of hydrostatic and deviatoric stress/strain components to damage, the above potential is separated into two parts and written as

$$\begin{aligned} A = {} & \frac{1}{2}(e_{uv} K_{uvst} e_{st} + \varepsilon_m \delta_{uv} K_{uvst} e_{st} + \varepsilon_m e_{uv} K_{uvst} \delta_{st}) \\ & + \frac{1}{2}\varepsilon_m^2 \delta_{uv} K_{uvst} \delta_{st} \end{aligned} \tag{19}$$

with e_{uv} (or e_{st}) the deviatoric strain tensor, $\varepsilon_m = (\varepsilon_{11} + \varepsilon_{22} + \varepsilon_{33})/3$ the mean strain, and δ_{uv} (or δ_{st}) the identity tensor (Kronecker's delta).

Considering the stiffness degradation induced by material damage and the different contribution of hydrostatic and deviatoric components to damage, Eq. (19) becomes

$$\begin{aligned} A = {} & \frac{1}{2}(1 - D)(e_{uv} K^0_{uvst} e_{st} + \varepsilon_m \delta_{uv} K^0_{uvst} e_{st} \\ & + \varepsilon_m e_{uv} K^0_{uvst} \delta_{st}) + \frac{1}{2}(1 - D\beta)\varepsilon_m^2 \delta_{uv} K^0_{vust} \delta_{st} \\ = {} & \frac{1}{2}(1 - D)\varepsilon_{uv} K^0_{vust} \varepsilon_{st} + \frac{(1 - \beta)D}{2}\varepsilon_m^2 \delta_{uv} K^0_{vust} \delta_{st} \end{aligned} \tag{20}$$

in which K^0_{uvst} is the initial secant constitutive tensor of the virgin material, D is a combined tension/compression damage parameter, and β a damage multiplier to reduce the susceptibility of the hydrostatic part to damage.

3.2. Damage parameters

It is widely recognised that the tensile and compressive strengths of concrete are significantly different. When concrete is subjected to a bi-axial or reverse cyclic loading, both tensile and compressive damage can occur. Therefore, two damage variables D_t and D_c are required for tensile and compressive damage, respectively. In addition, as stated earlier, convergence problems can be often induced when two damage surfaces conflict with each other. To tackle this problem a combined damage parameter is used, in which tensile and compressive damage parameters are weighted in the form

$$D = \frac{\sum \sigma_p^+ D_t + \sum |\sigma_p^-| D_c}{\sum |\sigma_p|} \tag{21}$$

where σ_p^+ and σ_p^- denote the positive and negative parts of the principal stress tensor, respectively; $\sum|\sigma_p|$ is the sum of the absolute values of the principal stresses. This definition implies that damage under uniaxial loading is governed by the corresponding damage parameter, while under bi-axial loading two damage parameters, D_t and D_c, both contribute to the induced damage. The effective contribution is in proportion to the ratio of positive and negative parts to the sum of absolute values of the principal stresses. The effect is equivalent to

separating the stress tensor into positive and negative two parts, but it simplifies considerably the implementation in a FE code and reduces the numerical difficulties.

Based on the failure characteristics of concrete, we assume the effect of the hydrostatic component on damage is less than that of the deviatoric component, and the damage multiplier (or damage reduction factor) β is designed to provide this reduction. Clearly, β is less than or equal to one. For the uniaxial version, the damage multiplier is defined as the ratio of the average stress σ_m to the maximum principal stress σ_1, i.e.

$$\beta = \left|\frac{\sigma_m}{\sigma_1}\right| \tag{22}$$

Under bi-axial loadings the response of concrete is dependent on the stress ratio, but it is not so easy to work out a straightforward relationship between damage and stress ratios. Moreover, whatever stress ratios are, it is no doubt that material damage is the consequence of energy dissipation in the damage mechanics point of view. Hence, the bi-axial version of the damage multiplier is proposed to be a damage energy release rate Y dependent parameter. In principle, the different mathematical forms of the damage multiplier can be assumed as long as they can match the corresponding experimental data well. In an initial attempt, a simple version is defined as

$$\beta = 1 - \frac{1}{1 + cY\mathrm{e}^{-dY}} \tag{23}$$

where e is the base of natural logarithms, and c and d can be regarded as two material constants to make β dimensionless and be so determined as to match experimental data in most cases. For the examples in this paper, values of $c = 2.0\ \mathrm{MPa}^{-1}$ and $d = 0.7\ \mathrm{MPa}^{-1}$ were adopted and provided acceptable results. However, it is worth mentioning that due to the complex behaviour of concrete subjected to different loading ratios, a more satisfactory form of the reduction factor β still warrants further study, especially for the case of combination of tension and compression.

3.3. Constitutive laws and damage surfaces

Based on the thermodynamics framework, the material constitutive relation and elasticity modulus can be now specified. Substituting Eq. (20) into Eqs. (12) and (13), the thermodynamic forces, Y_t and Y_c for tension and compression, respectively, and the stress tensor are derived as follows:

$$Y_t = \frac{\partial A}{\partial D_t} = \frac{\sum \sigma_p^+}{2\sum|\sigma_p|}\left[\varepsilon_{uv}K^0_{uvst}\varepsilon_{st} - (1-\beta)\varepsilon_m^2\delta_{uv}K^0_{uvst}\delta_{st}\right] \tag{24}$$

$$Y_c = \frac{\partial A}{\partial D_c} = \frac{\sum|\sigma_p^-|}{2\sum|\sigma_p|}\left[\varepsilon_{uv}K^0_{uvst}\varepsilon_{st} - (1-\beta)\varepsilon_m^2\delta_{uv}K^0_{uvst}\delta_{st}\right] \tag{25}$$

$$\sigma_{ij} = \frac{\partial A}{\partial \varepsilon_{ij}} = (1-D)K^0_{ijst}\varepsilon_{st} + \frac{(1-\beta)D\varepsilon_m}{3}\delta_{ij}\delta_{uv}K^0_{uvst}\delta_{st} \tag{26}$$

Since no plastic strain is taken into account in the model, the material constitutive law can be readily obtained from Eq. (26)

$$\dot{\sigma}_{ij} = K^t_{ijkl}\dot{\varepsilon}_{kl} \tag{27}$$

with

$$K^t_{ijkl} = (1-D)K^0_{ijkl} + \frac{(1-\beta)D}{9}\delta_{ij}\delta_{kl}\delta_{uv}K^0_{uvst}\delta_{st} \tag{28}$$

where D is corresponding to the new stress state at iteration $n+1$, i.e. $D = D^{n+1} = D^n + \Delta D$.

Since the magnitude of the damage energy release rate is a measure of how susceptible the material is to damage, it is used to define the damage criteria. Thus, the damage surfaces are described in the following forms for tensile and compressive damage, respectively:

$$f_t(Y_t, D_t) = Y_t - Z_t = 0 \tag{29}$$

$$f_c(Y_c, D_c) = Y_c - Z_c = 0 \tag{30}$$

where the hardening/softening parameters Z_t and Z_c are expressed as

$$Z_t = Y_t^0 + \frac{1}{a_t}\left(\frac{D_t}{1-D_t}\right)^{1/b_t} \tag{31}$$

$$Z_c = Y_c^0 + \frac{1}{a_c}\left(\frac{D_c}{1-D_c}\right)^{1/b_c} \tag{32}$$

in which parameters a_t and b_t are determined from a simple uniaxial tensile test, while a_c and b_c from a uniaxial compressive test. Their effects on Z have been explained in the preceding section. The initial values of damage energy release rates, Y_t^0 and Y_c^0, are material constants, specifying respectively the thresholds of tensile and compressive damage onset.

3.4. Implementation of the model

The implementation of this model is relatively simple, since the formulae are derived in strain-space and no inelastic deformation is considered at the current version. Since the items of $\sum|\sigma_p^+|/\sum|\sigma_p|$ and $\sum|\sigma_p^-|/\sum|\sigma_p|$ in Eqs. (24) and (25) are artificially defined stress ratios relative to positive and negative principal stresses, we assume that they only depend on the initial strain state of each increment. In doing so, the iterative scheme

is greatly simplified. The detailed algorithm is listed below, where the state at the start of a loading increment is denoted as n, and the end state as $n+1$.

1. Evaluate energy release rate for both tension and compression, respectively:

   Y_t^{n+1} and Y_c^{n+1}.

2. Check tensile damage.
   2.1 Check if current damage condition is violated:

   IF $f_t^{n+1}(Y_t^{n+1}, Z_t^n) = 0$,
   THEN $\Delta D_t = 0$, GOTO 4.

   2.2 Calculate ΔD_t, and update D_t and Z_t:

   $D_t^{n+1} = D_t^n + \Delta D_t$ and Z_t^{n+1}.

   2.3 Check if the evolution law at $n+1$ is satisfied:

   $f_t^{n+1}(Y_t^{n+1}, Z_t^{n+1}) = 0$.

   If false set $Z_t^n = Z_t^{n+1}$ and go to (2.2).
   Otherwise GOTO 5.
3. Check compressive damage.
   3.1 Check if current damage condition is violated:

   IF $f_c^{n+1}(Y_c^{n+1}, Z_c^n) \leqslant 0$,
   THEN $\Delta D_c = 0$, GOTO 4.

   3.2 Calculate ΔD_c, and update D_c and Z_c:

   $D_c^{n+1} = D_c^n + \Delta D_c$ and Z_c^{n+1}.

   3.3 Check if the evolution law at $n+1$ is satisfied:

   $f_c^{n+1}(Y_c^{n+1}, Z_c^{n+1}) = 0$.

   If false set $Z_c^n = Z_c^{n+1}$ and go to (3.2).
   Otherwise GOTO 5.
4. $D_t^{n+1} = D_t^n$ and/or $D_c^{n+1} = D_c^n$.
5. Evaluate total damage parameter $D(D_t, D_c)^{n+1}$.
6. Evaluate stress tensor σ_{ij}^{n+1}.
7. Evaluate tangential stiffness $(\partial\sigma_{ij}/\partial\varepsilon_{ij})^{n+1}$.
8. Evaluate the eigenvalue of stress tensor, σ_p^{n+1}.
9. Update parameters to new stress state:

$$\left(\sum \sigma_p^+ \Big/ \sum |\sigma_p|\right)^{n+1}, \quad \left(\sum \sigma_p^- \Big/ \sum |\sigma_p|\right)^{n+1},$$
$$\beta^{n+1}, \quad Z_t^{n+1} \text{ and } Z_c^{n+1}.$$

4. Application to concrete

The numerical algorithm of the proposed damage model has been developed and implemented [23] in the non-linear finite element code ABAQUS [26] via user subroutines. For evaluating its validity, several examples are performed under uniaxial and bi-axial loadings. Eight-noded quadratic plane stress elements are adopted. Loading is controlled by displacement to simulate the response of concrete in the softening regime. In order to compare with the experimental results of Karsan and Jirsa [27] and Gopalaratnam and Shah [28], the following material properties are used: Young's modulus 31.8 GPa, Poisson's ratio 0.18, maximum tensile strength 3.5 MPa, and maximum compressive strength −27.6 MPa. Eight model parameters were calibrated from the experimental data as: $a_t = 7000\ \text{MPa}^{-1}$; $b_t = 1.1$; $a_c = 29.0\ \text{MPa}^{-1}$; $b_c = 0.94$; $Y_t^0 = 1.9 \times 10^{-4}$ MPa; $Y_c^0 = 3.0 \times 10^{-4}$ MPa; $c = 2.0\ \text{MPa}^{-1}$; and $d = 0.7\ \text{MPa}^{-1}$, and used throughout this paper.

4.1. Uniaxial loading test

Fig. 5(a) and (b) illustrates the numerical results under uniaxial tension and compression, respectively. They are compared with the experimental data under tensile loading [28] and compressive loading [27]. There is a good agreement between the numerical and experimental data. However, an overestimation of the material tensile strength at the beginning of the softening branch is observed, which was caused by the proposed softening Eq. (15). It could be improved by fine-tuning of parameter b_t.

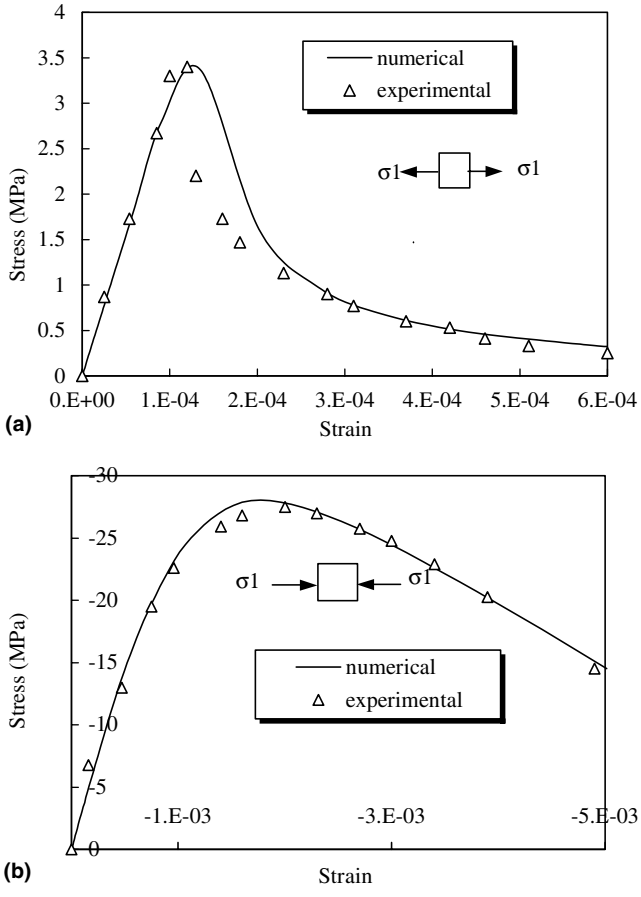

Fig. 5. Comparison of numerical solutions against experimental results: (a) uniaxial tension [28]; and (b) uniaxial compression [27].

4.2. Bi-axial loading test

The bi-axial loading tests are undertaken under different stress ratios. The numerical damage strengths of concrete are compared against three experimental failure surfaces of Kupfer et al. [29] in Fig. 6, where f_c donates the uniaxial compressive strength of concrete. It indicates that the numerical results are very close to the experimental ones, except that the equal bi-axial compressive strength is underestimated by approximately 5%. Note that the model constants for compression come from the uniaxial compressive curve of concrete with a compressive strength of 27.6 MPa, while the compressive strengths of three experimental groups denoted as *Kupfer-1*, *Kupfer-2* and *Kupfer-3* are 18.6, 30.9 and 32.1 MPa, respectively. Different types of concrete have different compressive curves, which may be one of the reasons for the induced errors.

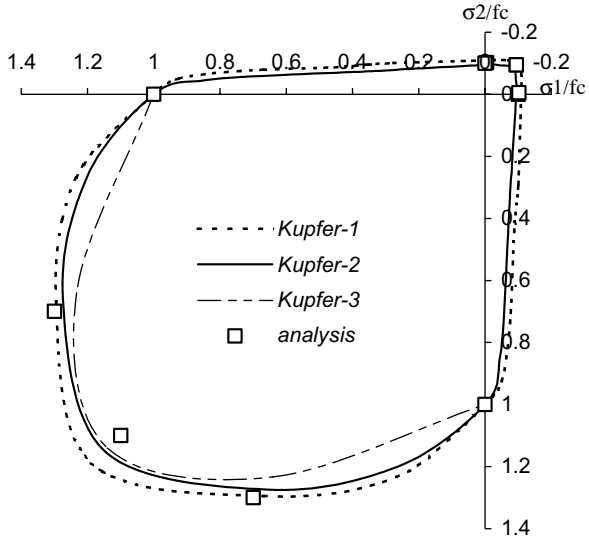

Fig. 6. Bi-axial strength of concrete.

Additionally, the proposed model is verified against the experimental results from Kupfer et al. under different stress ratios. Three tensile stress ratios (1/0, 1/1 and 1/0.55) and three compressive stress ratios (−1/0, −1/−1 and −1/−0.52) are tested and depicted in Figs. 7 and 8, respectively. Both tensile and compressive results present similar tendencies to the experiments. As we can see that a dependency exists in the second principal direction for the bi-axial stress ratio of 1:0.55, which, as expected, shows that a simple damage multiplier is not be powerful enough to accurately describe the behaviour of concrete in different bi-axial ratios. As for bi-axial compressive loads, there is, in general, an overestimation in strain. Although the difference between the concrete strengths used in the numerical analysis and those measured in the experiments is one of the causes of this overestimation, it is also the case that the single damage multiplier might not cope with both tensile and compressive. Similar results by Comi and Perego's fracture energy based bi-dissipative damage model [30] are plotted in the same graph. In their opinion, the absence of permanent strains in the model is a factor leading to underestimation of the peak strain for increasing lateral confinement.

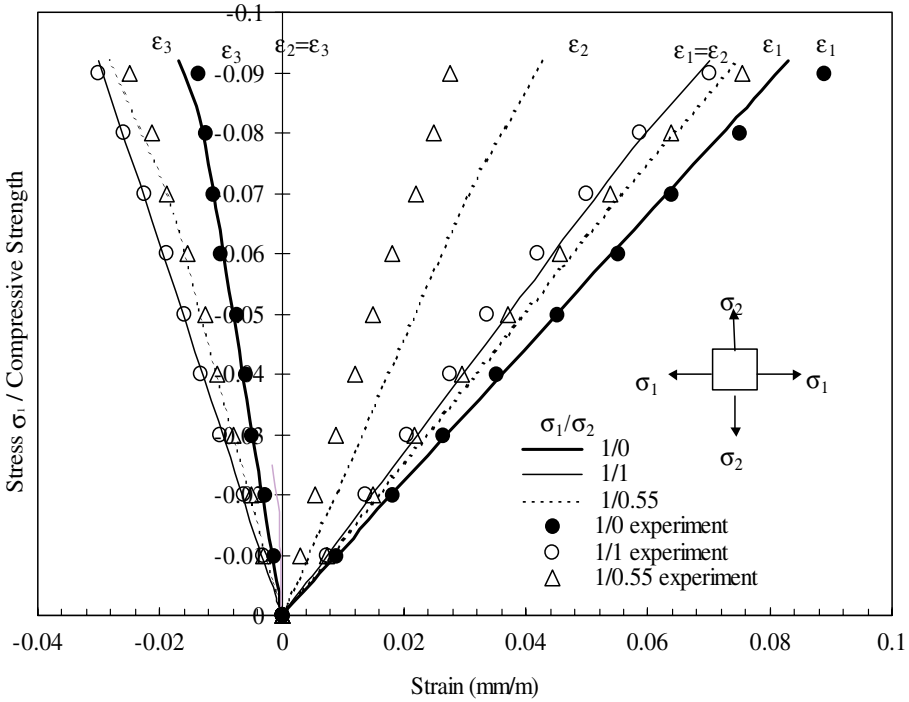

Fig. 7. Stress–strain relationships under bi-axial tension: (i) numerical results (lines); and (ii) experimental results [29] (symbols).

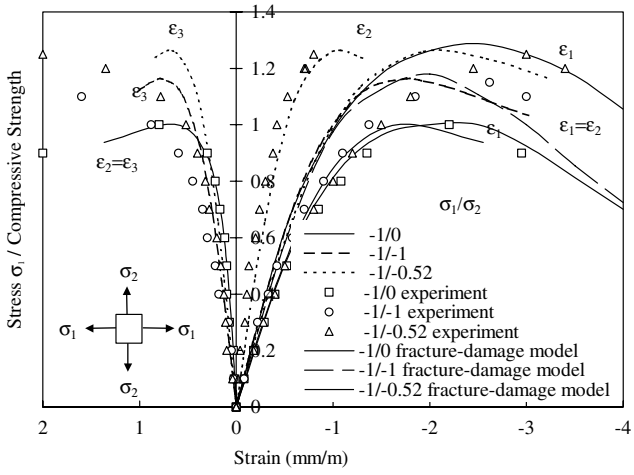

Fig. 8. Stress–strain relationships under bi-axial compression: (i) numerical results (thick lines); (ii) experimental results [29] (symbols); and (iii) fracture-damage model [30] (thin lines).

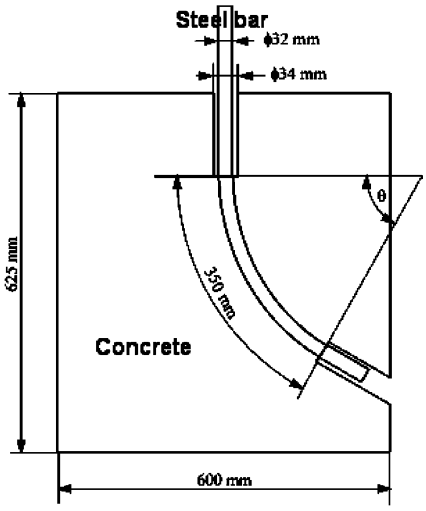

Fig. 10. Schematic diagram of test block.

4.3. Reverse cyclic loading test

Convergence has been recognised as a potential problem in developing the concrete model subjected to reverse cyclic loading. A conflict between tensile and compressive damage/failure surfaces arises with damage progress. A full cyclic loading path is conducted for the proposed model to test its convergence. The detailed loading path is shown in Fig. 9 and traces the labels o-a-o-b-o-c-d-o-e-f-o-g-h-o-i-j-o-k-l-o-m-n-o. Although it does not exhibit a real cycle response of concrete without residual deformation after unloading, satisfactory convergence was really achieved throughout as expected.

4.4. Pullout of bar reinforced concrete

In this example the proposed model is applied to simulate the pullout response of steel reinforced concrete.

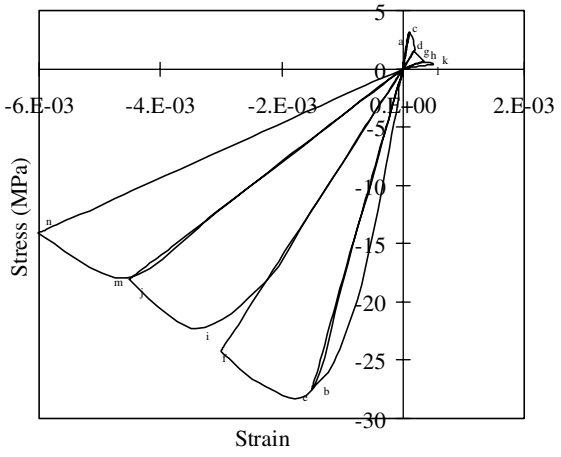

Fig. 9. Response of reverse cyclic loading.

As we know, a lot of pullout experiments on steel bar reinforced concrete have been carried out and reported. Amongst these the reinforcement used includes plain, deformed and anchored bars etc. As for numerical modelling, the curved and anchored bars have been troublesome in numerical convergence because of the severe damage of concrete that occurs in the vicinity of the bars.

In order to compare numerical solutions with the experimental results, we used similar size and material properties to those of Phillips et al. [31]. The dimension of the test block is illustrated in Fig. 10. Two shapes of steel bars are employed, one $\theta = 180°$ and the other $\theta = 90°$.

Eight-node quadratic plane strain elements are used for both bar and concrete. To reduce the number of elements, different mesh sizes are applied to concrete, with a finer mesh for the area close to the bars and a coarser mesh for the remaining parts. The mismatch of nodes between the two zones is dealt with by means of displacement constraint equations. Fig. 11 shows the detailed mesh and boundary conditions.

Due to a lack of corresponding uniaxial tensile and compressive test curves for the tested concrete, the same concrete is used as that in Sections 4.1–4.3. Table 1 lists the material parameters for both numerical model and experiment, where the subscripts c, s and u denote concrete, steel and ultimate strength, respectively. The behaviour of the interface between concrete and steel is described by a contact algorithm proposed by the authors [23].

The pullout responses are plotted in Fig. 12. It indicates that the model can reasonably predict the experimental observed behaviour. Fig. 13 shows the damage path in concrete. The critical damage zones are around the reinforcement and near supports.

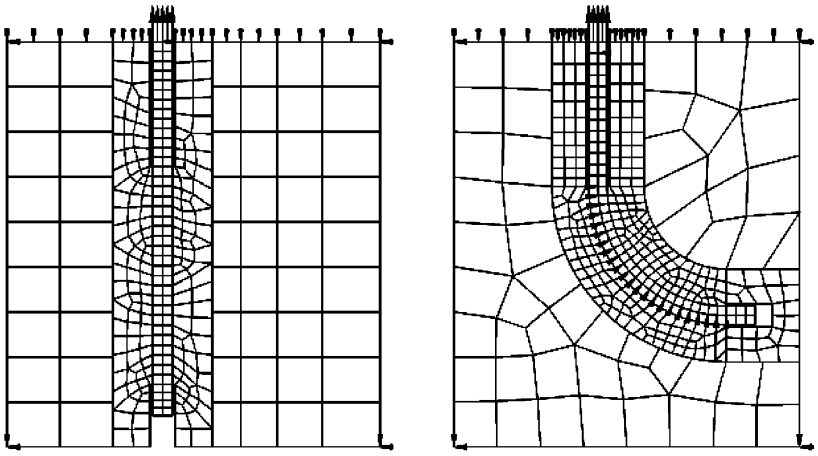

Fig. 11. Mesh and boundary conditions.

Table 1
Material properties used in analysis and experiment

	Model	Experiment
E_c	31.8 GPa	26.05 ~ 34.13 GPa
E_s	205.7 Gpa	205.7 Gpa
v_c	0.18	–
v_s	0.3	–
f_{cu}	34.8 MPa	46.5 ~ 54.1 MPa
f_{su}	455 MPa	455 Mpa

5. Conclusion

A simplified bi-axial damage model has been developed, which distinguishes between the contributions from hydrostatic and deviatoric components of the stress tensor to damage. Use of the weighted damage parameter and the so-called damage multiplier not only reduces the numerical difficulties, but it also enables a simple way to model bi-axial loading.

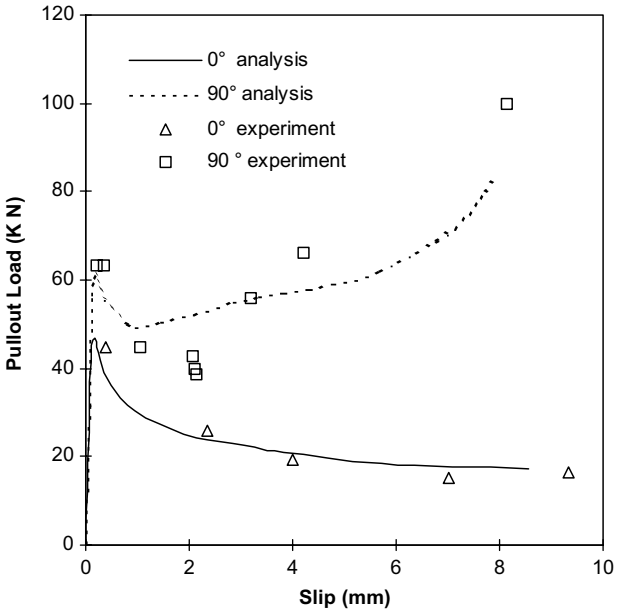

Fig. 12. Pullout responses (i) numerical results (lines); and (ii) experimental results [31] (symbols).

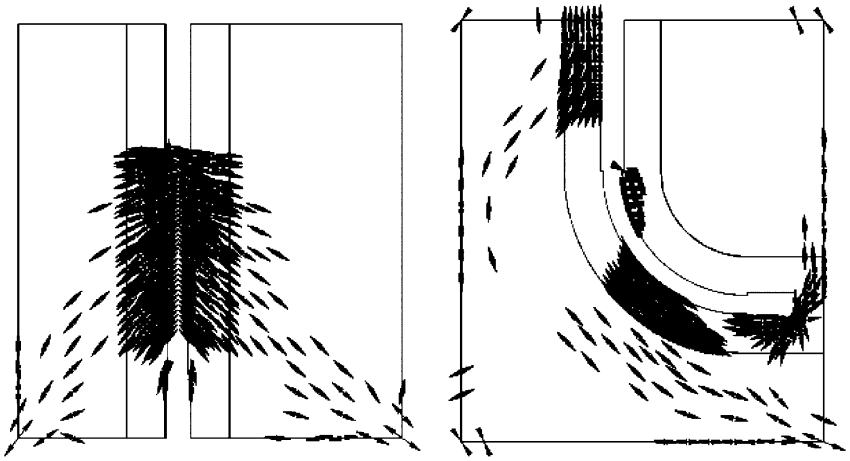

Fig. 13. Damage distribution under pullout load.

The paper illustrated that the proposed model is applicable to modelling concrete responses under monotonic, bi-axial loading and pullout load. The examples indicate that the numerical simulations agree reasonably with experimental data to a certain degree.

Since this model is based on an isotropic formulation of damage, the problems of strain localisation in the softening regime and consequent mesh dependence are inevitable, like most isotropic damage models, and some special features of concrete such as the dilation behaviour may not be captured. Therefore, adaptive meshing is suggested in finite element analysis to obtain more accurate results. On the other hand, the determination of the parameters c and d will influence computational accuracy under bi-axial loading. An extra attention has to be paid to the selection of them.

In summary, since this model does not include permanent strains, to capture complex, cyclic and non-proportional loading responses it should be coupled plasticity theory to account for irreversible frictional sliding at closed micro-cracks. However, it lays a foundation for further development. Importantly, it provides a simple and effective concrete model for uniaxial and bi-axial loading conditions and is easy to be incorporated into commercial and self-developed finite element software packages, especially for those applications where concrete suffers severe damage in local areas and large deformations, such as fibre or reinforcement pull out from a cement matrix. The model can be further enhanced by providing a more powerful form of the bi-axial damage multiplier, as well as by including plastic strains and crack closure.

References

[1] Ortiz M, Popov EP. Plain concrete as a composite material. Mech Mater 1982;1:139–50.
[2] Ortiz M. A constitutive theory for the inelastic behaviour of concrete. Mech Mater 1985;4:67–93.
[3] Yazdani S, Schreyer H. An anisotropic damage model with dilatation for concrete. Mech Mater 1988;7:231–44.
[4] La Borderie C, Mazars J, Pijaudier-Cabot G. Response of plain and reinforced concrete structures under cyclic loading. ACI SIP 1992;134:147–72.
[5] Simo JC, Ju JW. Strain- and stress-based continuum damage models formulation. Int J Solids Struct 1987;23(7):821–40.
[6] Lemaitre J. Coupled elasto-plasticity and damage constitutive equations. Comput Meth Appl Mech Eng 1985;51:31–49.
[7] Resende L. Damage mechanics constitutive theory for the inelastic behaviour of concrete. Comput Meth Appl Mech Eng 1987;60:57–93.
[8] Ju JW. On energy-based coupled elastoplastic damage theory: constitutive modelling and computational aspects. Int J Solids Struct 1989;25(7):803–33.
[9] Lubliner J, Oliver J, Oller S, Oñate E. A plastic-damage model for concrete. Int J Solids Struct 1989;25(3):299–326.
[10] Luccioni B, Oller S, Danesi R. Coupled plastic-damaged mode. Comput Meth Appl Mech Eng 1996;129:81–9.
[11] Faria R, Oliver J, Cervera M. A strain-based plastic viscous-damage model for massive concrete structures. Int J Solids Struct 1998;35:1533–58.
[12] Halm D, Dragon A. An anisotropic model of damage and frictional sliding for brittle materials. Eur J Mech—A/Solids 1998;17:439–60.
[13] Dragon A, Halm D, Désoyer Th. Anisotropic damage in quasi-brittle solids: modelling, computational issues and application. Comput Meth Appl Mech Eng 2000;183:331–52.
[14] Ragueneau F, La Borderie C, Mazars J. Damage model for concrete-like materials coupling cracking and friction, contribution towards structural damping: first uniaxial application. Mech Cohesive-Fract Mater 2000;5:607–25.
[15] Brencich A, Gambarotta L. Isotropic damage model with different tensile–compressive response for brittle materials. Int J Solids Struct 2001;38:5865–92.
[16] Gambarotta L. Friction-damage coupled model for brittle materials. Eng Fract Mech 2004;71:829–36.
[17] Mazars J. Application de la mécanique de l'endommangement au comportement non linéaire et à la rupture du béton de structure. Technical report, LMT, France: Université Paris; 1984.
[18] Thionnet A, Renard J. Modelling unilateral damage effect in strongly anisotropic materials by the introduction of the loading mode in damage mechanics. Int J Solids Struct 1999;36:4269–87.
[19] Mazars J, Pijaudier-Cabot G. Continuum damage theory application to concrete. J Eng Mech, ASME 1989;115(2):345–65.
[20] Fichant S, Pijaudier-Cabot G, La Borderie C. Continuum damage modelling with crack induced anisotropy. In: Owen DRJ, editor. Proc of Complas 4, vol. 1. p. 1045–56.
[21] Baker G, de Borst R. A thermo-mechanical damage model for concrete at elevated temperatures. In: Wittmann FH, editor. Proceedings FRAMCOS-2, London. p. 991–1000.
[22] Nechnech W, Meftah F, Reynouard JM. An elastoplastic damage model for plain concrete subjected to high temperature. Eng Struct 2002;24:597–611.
[23] Tao XY. Pullout behaviour of steel reinforced cement composites. PhD thesis. Glasgow, UK: Department of Civil Engineering, University of Glasgow; 2000.
[24] Phillips DV, Tao XY. Numerical modelling of pullout of curved bars in reinforced concrete. In: The 8th Conference of ACME, London. p. 123–6.
[25] Kachanov LM. On the creep fracture time. Izv AN SSR, Otd Tekhn Naukin 1958:26–31. [Russian].
[26] Karlsson, Hibbitt, Sorensen. ABAQUS: Theory Manual Version 5.6. Hibbitt, Karlsson and Sorensen Inc.; 1996.
[27] Karsan ID, Jirsa JO. Behaviour of concrete under compressive loadings. J Struct Div, ASCE 1969;95(12):2535–63.
[28] Gopalaratnam VS, Shah SP. Softening response of plain concrete in direct tension. ACI, J 1985;82(3):310–23.
[29] Kupfer H, Hilsdorf HK, Rusch H. Behaviour of concrete under bi-axial stresses. ACI J 1969;66(8):656–66.
[30] Comi C, Perego U. Fracture energy based bi-dissipative damage model for concrete. Int J Solids Struct 2001;38:6427–54.
[31] Phillips, DV, Green, DR, Zhang, B, Scott, RH. Bond behaviour in curve bars under monotonic & cyclic loading. Department of Civil Engineering Research Report, No. CE-ST95-54, Glasgow University; 1995.